Available online at www.sciencedirect.com
SCIENCE DIRECT®
Thermochimica Acta 403 (2003) 207–218
thermochimica acta
www.elsevier.com/locate/tca

Carbochlorination of samarium sesquioxide

M.R. Esquivel [a,*], A.E. Bohé [b], D.M. Pasquevich [a,b]

[a] *Comisión Nacional de Energía Atómica, Centro Atómico Bariloche, 8400 San Carlos de Bariloche, Río Negro, Argentina*
[b] *Consejo Nacional de Investigaciones Científicas y Técnicas, Centro Atómico Bariloche, 8400 San Carlos de Bariloche, Río Negro, Argentina*

Received 5 November 2002; accepted 19 December 2002

Abstract

The chlorination of Sm_2O_3 in the presence of carbon using the gaseous mixture $Cl_2(g) + Ar(g)$ has been studied by thermogravimetry. The effects of both the temperature between 200 and 950 °C and the total gas flow rate between 2.1 and 7.9 l h^{-1} on the reaction rate were analyzed. The starting temperature of reaction, the stoichiometry and kinetic regimes of the reaction were obtained. Reactants and products were analyzed by X-ray diffraction (XRD) and electronic dispersive spectroscopy (EDS). The temporal evolution of the solid microstructure was followed by scanning electron microscopy (SEM).

Keywords: Samaria; Thermogravimetry; Gas–solid; Carbochlorination

1. Introduction

Like the other lanthanide elements, Samarium possesses a stable trivalent state [1,2] which determines its main stable oxide, Sm_2O_3 [3,4]. These compounds are among the most stable in nature [4]. This feature, along with the chemical similarities exhibited by all the lanthanide sesquioxides [1,2,5], makes difficult either their extraction from the mineral [5,6] or the separation from synthetic mixtures [5,6]. Since the direct chlorination of the lanthanide sesquioxides is thermodynamically feasible over 400 °C [7], it provides a suitable method for the production of the chloride [5]. But the global reaction releases oxygen which may react with the obtained chloride to form an oxychloride instead. Therefore, the chlorination of Sm_2O_3 to produce its chlorides is achieved in the presence of carbon.

This compound plays two roles in the reaction:

(1) *Thermodynamic*: Carbon provides a low oxygen potential atmosphere, diminishing the potential of the oxide and favoring the formation of the chloride [8].
(2) *Kinetic*: Carbon is thought to favor the formation of reaction intermediates producing an increment in both the maximum reaction degree achieved at a given time and an increase on the reaction rate [8,9].

Changes on the carbon surface are observed if carbon is reacted in a given oxide–chlorine system [8,9]. No changes on carbon are seen if the direct chlorination between chlorine and oxide is achieved.

The chlorination of Sm_2O_3 in the presence of carbon to produce its chlorides represents an important technological subject and a method of separation of lanthanide oxides at high temperatures (1200 °C) has

* Corresponding author. Tel.: +54-29-4444-5397; fax: +54-29-4444-5100.
E-mail address: esquivel@cab.cnea.gov.ar (M.R. Esquivel).

0040-6031/03/$ – see front matter © 2003 Elsevier Science B.V. All rights reserved.
doi:10.1016/S0040-6031(03)00047-9

Nomenclature

D	diffusion coefficient ($m^2\,s^{-1}$)
E_{ap}	apparent activation energy ($kJ\,mol^{-1}$)
L	characteristic dimension of the sample (m)
m_0	initial mass sample (mg)
Δm	mass variation (mg)
ΔM	balance mass variation (mg)
N	molar flow of chlorine ($mol\,s^{-1}$)
P	pressure (kPa)
r	reaction rate ($mol\,s^{-1}$)
R	reaction rate (s^{-1})
t	time (s)
T	temperature (°C)
W	formula weight ($kg\,mol^{-1}$)

Greek symbols

α	Sm_2O_3 reaction degree (dimensionless)
β	stoichiometric coefficient (dimensionless)
ν	kinematic viscosity ($m^2\,s^{-1}$)

been reported [10]. Despite that and the academic importance, the effect of temperature and total gas flow rate on the carbochlorination of Sm_2O_3 has not been studied to the best of the author's knowledge. This situation has aimed the elaboration of the present paper.

2. Experimental

2.1. Materials and procedure

Gases used were Ar 99.999% purity (AGA, Argentina) and Cl_2 99.8% (Indupa, Argentina). Solid reactants utilized were Sm_2O_3 and carbon. Both substances were previously characterized [6,11]. Carbon was obtained from the calcination of sucrose (Fluka Chemie AG) in inert atmosphere at 980 °C during 48 h and sieved to a size of −200 to 275 mesh (ASTM) [11]. Carbon characteristics are given elsewhere [11]. Since Sm_2O_3 absorbs either CO_2 or H_2O from atmosphere [12], it was previously burned at 950 °C [3,4]. Sm_2O_3 possesses a particle distribution between 5 and 20 μm as observed by scanning electron microscopy (SEM) and a BET surface area of $6.571 \pm 0.0389\,m^2\,g^{-1}$. Sm_2O_3 structure was verified by comparing the experimental lines with those contained on PDF-1 (1996) [13] using PC Identify program (PW1776). Masses of these reactants were weighed and mixed mechanically to obtain a mixture of Sm_2O_3–C 10.58 wt.% of carbon.

The measurements were performed on a thermogravimetric analyzer based on a Cahn 2000 electrobalance adapted to work with corrosive atmospheres. The system is described elsewhere [14]. The mass change resolution of the system was of ±10 μg under the experimental conditions [8,11,14]. Samples were placed inside a quartz crucible suspended by a quartz fiber inside a furnace. Isothermal and non-isothermal measurements were made.

In the first ones, samples were heated for 1 h in Ar atmosphere at the desired operation temperature. After that, Cl_2 was injected into the system reaching a $p_{Cl_2} = 30.3$ kPa under a overall pressure of 101.3 kPa. The total gas flow rate was varied between 2.1 and $7.9\,l\,h^{-1}$.

In the second ones, samples were heated from room temperature to 950 °C at $2.6\,°C\,min^{-1}$ at a $p_{Cl_2} = 30.3$ kPa in flowing Ar–Cl_2 under a overall pressure of 101.3 kPa. In both cases, mass changes were measured and apparent mass changes were corrected as explained elsewhere [8,11,14]. Since $SmCl_3$ is hygroscopic [1,15], auxiliary measurements were made [6,7]. Samples obtained were isolated and handled inside a glove box [6,7].

2.2. Expression of results

For non-isothermal runs, TG data is expressed as ΔM versus T, where ΔM is the experimental mass change observed and T is the temperature in degree Celsius (°C). For isothermal runs, TG data is expressed as the fractional oxide mass loss given by $\alpha = \Delta m(Sm_2O_3)/m_0(Sm_2O_3)$, where $\Delta m(Sm_2O_3)$ is the Sm_2O_3 mass loss and $m_0(Sm_2O_3)$ is the initial Sm_2O_3 mass. Sm_2O_3 consumption is related to the observed mass change by $\Delta m(Sm_2O_3) = \beta\,\Delta M$.

Where β and ΔM stand for the different stoichiometries involved and observed mass loss, respectively. Therefore, the reaction degree is transformed to:

$$\alpha = \left(\frac{\beta\,\Delta M}{m_0(Sm_2O_3)}\right) \quad (1)$$

The reaction rate (s^{-1}) is then:

$$R = \left(\frac{da}{dt}\right) = -\left[\frac{\beta}{m_0(Sm_2O_3)}\right]\left(\frac{dM}{dt}\right) \quad (2)$$

The reaction rate (mol Cl_2 s^{-1}) is:

$$r = \left(\frac{dn(Cl_2)}{dt}\right) = \left[\frac{m_0(Sm_2O_3)}{W(Sm_2O_3)}\right]R \quad (3)$$

where $n(Cl_2)$ are moles of Cl_2 and $W(Sm_2O_3)$ is the formula weight of Sm_2O_3.

3. Results and discussion

3.1. Thermodynamics

In the 20–950 °C temperature range, $SmCl_2$(s), $SmCl_3$(s) and SmOCl(s) [15–17] are the possible reaction products of the carbochlorination of Sm_2O_3. Liquid and gaseous chlorides are also probable because $SmCl_3$ and $SmCl_2$ have mp of 681 and 752 °C, respectively [17]. These compounds can be produced along with O_2(g), CO(g) and CO_2(g) during the carbochlorination.

A thermodynamic analysis was performed [18] to estimate the probable reaction products. Calculations considering masses of chlorine and carbon in excess over the stoichiometric consumption of Sm_2O_3 in a molar ratio of 4/4/1 were performed at five representing temperatures: 300, 550, 650, 750 and 950 °C. The main reaction products are shown in Table 1.

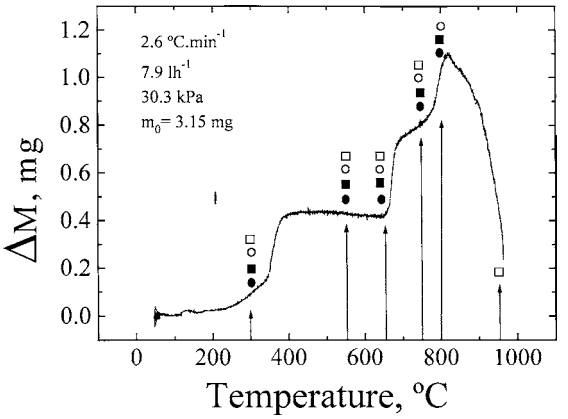

Fig. 1. Non-isothermal curve of the carbochlorination of Sm_2O_3. Selected temperatures of analysis are indicated by arrows. XRD and EDS techniques are indicated by hollow and full circles, respectively. Thermodynamic calculations and SEM observations are indicated by full and hollow squares, respectively.

3.2. Preliminary analysis

Non-isothermal exploratory measurements were made to determine both the reactivity with temperature and the main products of the Sm_2O_3–C–Cl_2 system. The thermogravimetric curve is displayed in Fig. 1. Corrections to the curve were made as indicated

Table 1
Reaction products with carbon and Cl_2 in excess (Sm_2O_3–C–Cl_2 in a initial 4/4/1 molar ratio)

Compounds in equilibrium	300 °C	550 °C	650 °C	750 °C	950 °C
Condensed phase (mol)					
C(s)	2.499	2.364	2.015	1.454	1.031
$SmCl_3$(s)	1.934	1.409	1.084	1.000	1.000
$SmCl_2$(s)	–	–	–	–	–
SmOCl(s)	–	–	–	–	–
Sm_2O_3(s)	–	–	–	–	–
$SmCl_2$(l)	–	–	–	–	–
$SmCl_3$(l)	0.065	0.509	0.916	0.999	0.999
Gaseous phase (mol)					
CO(g)	0.001	0.271	0.968	2.090	2.937
CO_2(g)	1.449	1.364	1.015	0.455	0.031
Cl_2(g)	1.000	1.000	1.000	1.000	1.000
$SmCl_3$(g)	–	–	–	–	–
$SmCl_2$(g)	–	–	–	–	–
O_2(g)	–	–	–	–	–

elsewhere [14]. From 200 to 825 °C, the mass is incremented as temperature is increased. Flat and steeped zones are alternatively seen along the curve. Different condensed products of reaction are formed in each zone. Over 825 °C, a mass loss associated to either a gasification reaction [7] or a vaporization process of a condensed phase [7] is observed.

3.3. Effect of the temperature: products of reaction and stoichiometry

To determine the identity of the compounds observed in Fig. 1, isothermal experiments at five characteristic temperatures, 300, 550, 650, 750 and 800 °C, were made. These are indicated by solid arrows. The samples were led to react at different reaction degrees and analyzed by X-ray diffraction (XRD), electronic dispersive spectroscopy (EDS) and SEM as indicated in Fig. 1 by hollow circles, full circles and full squares, respectively. Hollow squares correspond to the thermodynamic calculations indicated in Table 1.

3.3.1. Analysis from 200 to 375 °C

A XRD diffractogram of the products of reaction at 300 °C is shown in Fig. 2A. For comparison, the reference pattern of SmOCl [19] is shown in Fig. 2C.

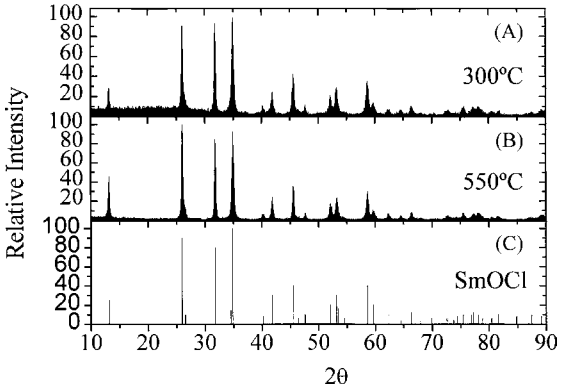

Fig. 2. Diffraction patterns of the reaction products: (A) 300 °C; (B) 550 °C; (C) reference pattern of SmOCl [19].

No diffraction lines other than SmOCl are observed. A SEM image of the products at this temperature is shown in Fig. 3. The plate-like particles grouped into chunks correspond to SmOCl identified by EDS microanalysis. Smooth steeped particles correspond to carbon. These particles are labeled in the figure. No attacks on carbon surface, such as channeling or pitting are observed [8,9]. Mass balances calculated from TG curves performed on the 200–375 °C range are in agreement with the formation of solid SmOCl

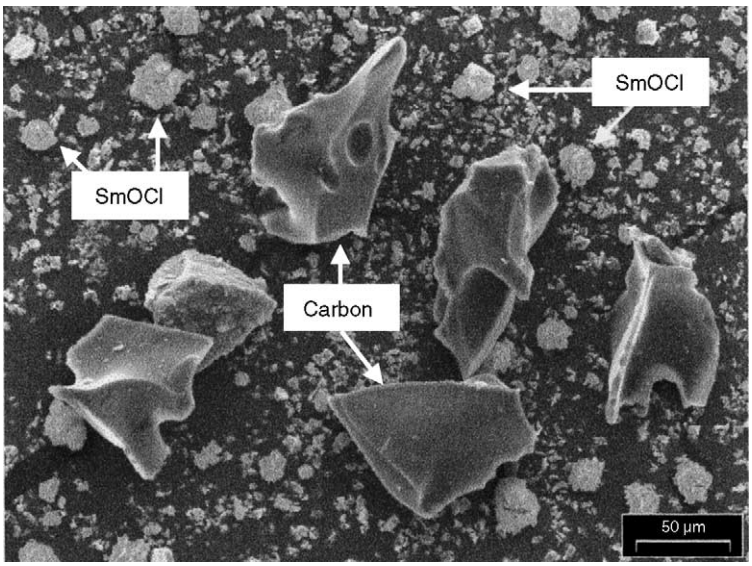

Fig. 3. SEM image of the reaction products at 300 °C. Carbon surface presents no attacks. SmOCl, plate-like particles grouped in chunks, are identified by EDS.

according to:

$$Sm_2O_3(s) + Cl_2(g) \rightarrow 2SmOCl(s) + \tfrac{1}{2}O_2(g) \quad (4)$$

Therefore, carbon is not involved on the reaction. The stoichiometry of Eq. (4) corresponds to the direct chlorination of Sm_2O_3 [20]. This system is analyzed elsewhere [20].

3.3.2. Analysis from 400 to 625 °C

Five hundred and fifty degree Celsius was selected as the temperature representative of this range. The XRD diffractogram of the reaction products at that temperature is shown in Fig. 2B. SmOCl [19] is the reaction product observed. A SEM image detailing the carbon surface is displayed in Fig. 4. The small chunks resting on the carbon surface are SmOCl particles. The carbon surface does present chemical attacks [8,9,21]. Then, its participation on the reaction is evidenced [8,9,21]. This is in agreement with previous observations indicating that this type of carbon is feasible of being oxidized over 400 °C [11,22]. The mass balances performed on the TG curves in the 400–625 °C range are in agreement with the following reaction:

$$Sm_2O_3(s) + \tfrac{1}{2}C(s) + Cl_2(g) \rightarrow 2SmOCl(s) + \tfrac{1}{2}CO_2(g) \quad (5)$$

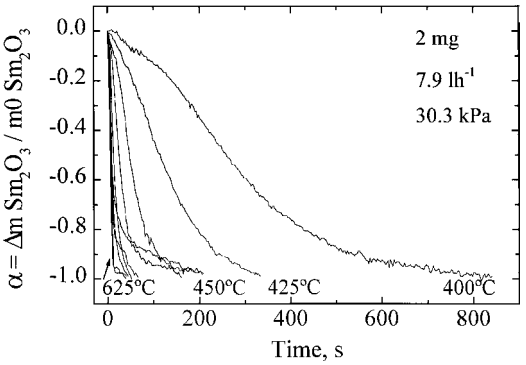

Fig. 5. Effect of the temperature for 2 mg of $Sm_2O_3 + C$ in the 400–625 °C temperature range.

The corresponding TG curves are shown in Fig. 5. The carbochlorination at all temperatures is fully achieved. The reaction rate is increased as temperature is raised. Carbochlorination is fulfilled in the order of 1×10^3 and 25 s at 400 and 625 °C, respectively. As observed in Fig. 5, the TG curves become closer to each other as temperature is incremented over 450 °C.

3.3.3. Analysis from 650 to 725 °C

Fig. 6 is a SEM image of the reaction products at 650 °C. Pitting is observed at carbon surface [8,9,21]

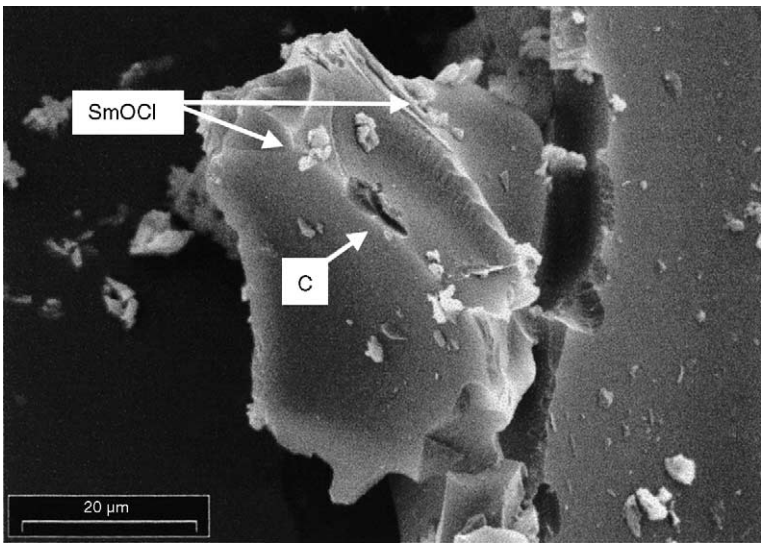

Fig. 4. SEM image of the reaction products at 550 °C. Attacks on carbon surface are observed. Small particles are SmOCl identified by EDS.

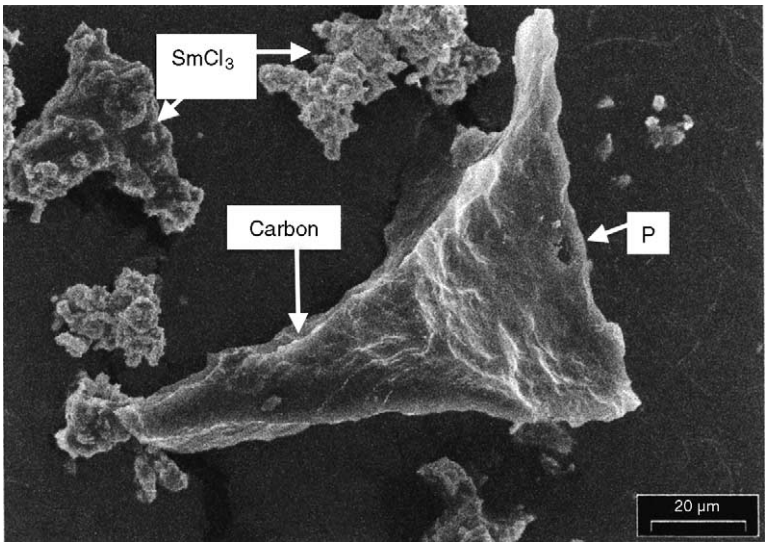

Fig. 6. SEM image of the reaction products at 650 °C. Pitting on carbon surface is indicated by the letter "P". $SmCl_3$ identified by EDS is also indicated.

and is indicated by the letter "P". Particles of $SmCl_3$ identified by EDS are also indicated by arrows. The isothermal TG curves performed in this temperature range are shown in Fig. 7. Unlike the lower temperatures, the curves present significant discontinuities attributed to two stages. The first one is quickly achieved in the first 20 s of reaction at all temperatures. The diffractogram showing the reaction products at this stage at 650 °C is displayed in Fig. 8A. For comparison, the reference pattern of SmOCl [19] is displayed

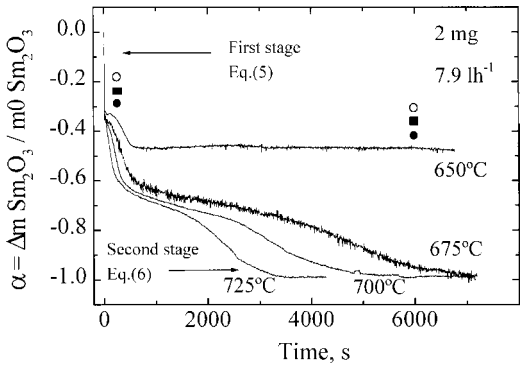

Fig. 7. Effect of the temperature for 2 mg of $Sm_2O_3 + C$ in the 650–725 °C temperature range. Techniques used to analyze samples at each stage are indicated by its symbol.

in Fig. 8B The mass balances performed in this stage, are in agreement with the formation of SmOCl according to Eq. (5).

The second stage rate is slower than the first, i.e. the first stage is fully achieved in 18 s and the second stage is finished at 5.5×10^3 s at 700 °C. A diffractogram of the products of reaction at this stage at 650 °C is displayed in Fig. 8C. For comparison, the reference pattern of $SmCl_3$ [23] is displayed on Fig. 8D. By comparing the experimental diffractograms and those of the reference is inferred that the product of reaction is a mixture of the SmOCl formed at the first stage and $SmCl_3$ produced in the second stage. Over 650 °C and up to 700 °C, the global mass balances including both the first and second stage are in agreement with the following reaction:

$$Sm_2O_3(s) + \tfrac{3}{2}C(s) + 3Cl_2(g) \rightarrow 2SmCl_3(s, l) + \tfrac{3}{2}CO_2(g) \quad (6)$$

Mass balances performed at 725 °C indicates that the reaction at this temperature presents a global stoichiometry with values closer to both that of Eq. (6) and that of the following:

$$Sm_2O_3(s) + 3C(s) + 3Cl_2(s) \rightarrow 2SmCl_3(s, l) + 3CO(g) \quad (7)$$

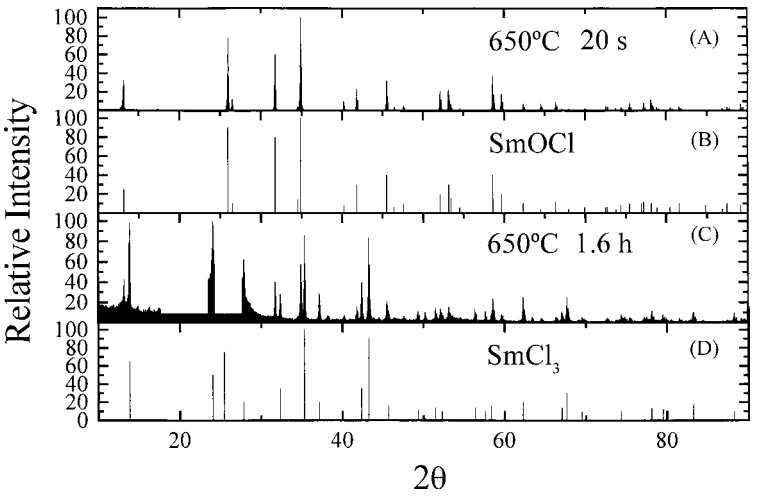

Fig. 8. Diffraction patterns of the reaction products at 650 °C; (A) 20 s of reaction; (B) reference pattern of SmOCl [19]; (C) 1.6 h of reaction; (D) reference pattern of $SmCl_3$ [23].

3.3.4. Analysis from 750 to 950 °C

The isothermal thermogravimetric curves corresponding to this temperature range are displayed on Fig. 9. Two successive stages are detected. Like the previous temperature range analyzed, the first one is quickly and fully achieved in the order of 20 s at all temperatures. The second one is slower and fulfilled in 150 s at 950 °C, the higher temperature.

The diffraction patterns of the reaction products are not shown here, but the products of reaction are also SmOCl and $SmCl_3$ in the first and second stages, respectively.

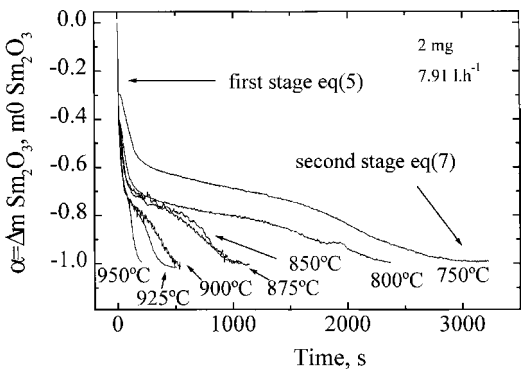

Fig. 9. Effect of the temperature for 2 mg of $Sm_2O_3 + C$ in the 750–950 °C temperature range.

A SEM image showing the reaction products at 750 °C is displayed on Fig. 10. A strong chemical attack is clearly observed at the carbon surface where both pitting [8,9,22] and channeling [8,9,22] are indicated by arrows. Letters "P" and "C" stand for pitting and channeling, respectively. The granular mass observed behind the carbon is molten $SmCl_3$ identified by EDS. Mass balances performed on the TG curves led to the conclusion that at temperatures between 750 and 850 °C the stoichiometry of the first stage is given by Eq. (5).

At temperatures higher than 850 °C, both the first stage and SmOCl are detected but no exact stoichiometry calculated by mass balances can be associated. In all temperature ranges, mass balance indicated that the global stoichiometry corresponds to Eq. (7).

3.4. The effect of the total gas flow rate

As usual in solid–gas reactions, the effect of the total gas flow rate on the reaction rate was analyzed [24]. Starvation [7,24] was studied by changing the flow rate from 2.1 to 7.9 l h^{-1} at two different temperatures: 400 and 950 °C. The TG curves are shown in Fig. 11A and B, respectively. No significant changes on the reaction rate are noticed at 400 °C when the total flow rate is increased. A slight increment is observed in both stages when the flow rate is incremented at 950 °C.

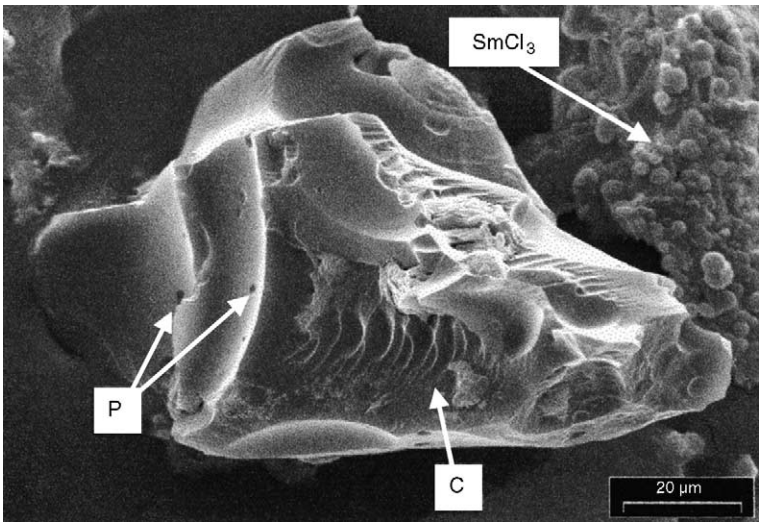

Fig. 10. SEM image of the reaction products at 750 °C. Both pitting and channeling are observed on the carbon surface and indicated by the letters "P" and "C". $SmCl_3$ identified by EDS is also indicated.

Therefore, starvation is thought to affect the reaction at the higher temperatures [7,24].

By comparing the effect of the total gas flow rate at both temperatures (Fig. 11) it is inferred that the effect of total gas flow rate is not uniform in all temperature ranges involved. It is reasonable because starvation is only one of the effects involved in external mass transfer.

The other effect to be studied is convective mass transfer [7,24]. It is done by comparing the experimental reaction values to those of theoretical equations [7,24] such as Ranz–Marshall [7,24]. The comparison is performed at two different reaction degrees at four different temperatures in Table 2. The reaction stoichiometries, D, and ν, the diffusion coefficient and the kinematic viscosity used to calculate the Ranz–Marshall equation, are also shown [7,24]. The experimental values at the low reaction degree become closer to those of the theoretical equation as temperature is raised over 550 °C. But the experimental values at the higher reaction degree, $\alpha = 0.5$, are at least two orders lower than the theoretical ones at temperatures higher than 650 °C. Therefore, the first stage of reaction is affected by convective mass transfer at temperatures over 550 °C. The second stage is not noticed to be influenced, not controlled, by convection at temperatures as high as 950 °C since its theoretical values are at least one order higher than the experimental ones. Despite that, this stage is affected by starvation as observed in Fig. 11B.

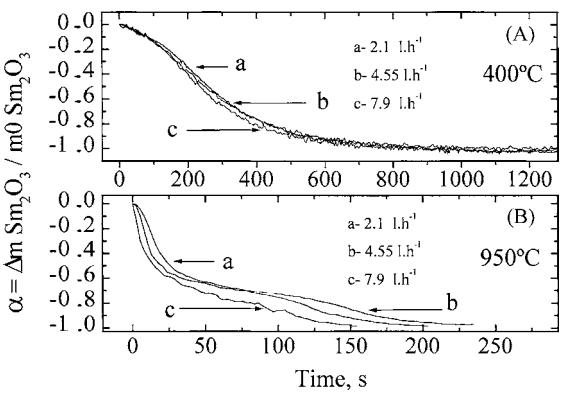

Fig. 11. Effect of the total gas flow rate on the carbochlorination of 2 mg of $Sm_2O_3 + C$: (A) at 400 °C; (B) at 950 °C.

3.5. The activation energy and regimes of reaction

3.5.1. The formation of SmOCl

As observed on Table 1, $SmCl_3$ is the most favored product of the carbochlorination at all temperatures [18]. Nevertheless, SmOCl is the only obtained product at temperatures below 650 °C. It may be due to the

Table 2
Comparison between r (experimental) and N (theoretical) rates

T (°C)	D (cm s^{-2})	ν (cm s^{-2})	N (mol Cl_2 s^{-2})	α	r stoichiometry	r (mol Cl_2 s^{-2})
550	0.68	0.61	4.10×10^{-7}	0.2	Eq. (5)	3.56×10^{-7}
				0.5	Eq. (5)	2.33×10^{-7}
650	0.83	0.74	4.57×10^{-7}	0.2	Eq. (5)	3.76×10^{-7}
				0.45	Eq. (6)	7.37×10^{-10}
750	1.00	0.89	5.28×10^{-7}	0.2	Eq. (5)	5.25×10^{-7}
				0.5	Eq. (7)	2.00×10^{-9}
850	1.18	1.04	5.90×10^{-7}	0.2	Eq. (5)	5.86×10^{-7}
				0.5	Eq. (7)	8.04×10^{-9}
950	1.21	1.21	7.50×10^{-7}	0.2	Eq. (7)	7.32×10^{-7}
				0.5	Eq. (7)	1.78×10^{-8}

Values of D and ν at various temperatures for $p_{Cl_2} = 30.3$ kPa. N values are calculated according to the Ranz–Marshall equation and corrected as suggested [7,25,28]. In this equation $L = 0.10$. The experimental values of r are obtained for 2 mg of $Sm_2O_3 + C$ under a $p_{Cl_2} = 30.3$ kPa and a total gas flow rate of 7.9 l h^{-1} at each temperature. The equation stoichiometry used to calculate r is indicated in the third column.

differences on the kinetics of formation of the oxychloride and the chloride. It appears to be consistent with the fact that the formation of $SmCl_3$ is accomplished after that of SmOCl at 650 °C. Between 400 and 625 °C, the further chlorination of the SmOCl to $SmCl_3$ would demand much more time than those at higher temperatures. Therefore, the product of the carbochlorination is SmOCl.

From 650 to 850 °C, the formation of SmOCl becomes the first step of the carbochlorination of the Sm_2O_3. It is achieved with the stoichiometry of Eq. (5). Over 850 °C, the SmOCl is also detected as the first reaction product but no exact stoichiometry is associated.

The calculation of the activation energy of the formation of SmOCl in the 400–850 °C range is displayed in Fig. 12. Between 400 and 525 °C, the lines are parallel at all reaction degrees indicating that the kinetic regime is the same. Despite only those of 0.1, 0.3, 0.5, 0.7 are shown, the apparent activation energy values (E_{ap}) obtained were calculated at α values between 0.1 and 0.9. The E_{ap} value found is of 120 ± 5 kJ mol^{-1}. This value suggests either mixed or chemical control [25]. Although the direct chlorination of Sm_2O_3 is also possible at this temperature range [20], its E_{ap} value between 375 and 950 °C is 12 ± 7 kJ mol^{-1} [20], one order lower than that found for the carbochlorination.

At 525 °C, the E_{ap} lines present a break in Fig. 12. The E_{ap} values calculated between 525 and 850 °C are of the order of 20 ± 10 kJ mol^{-1}. Although only those curves of $\alpha = 0.1$, 0.3, 0.5 and 0.7 are shown, the calculus were performed for α values between 0.1 and 0.9. This low E_{ap} value suggests external mass transfer control [25,26]. This conclusion is in agreement with Figs. 7 and 9 where the reaction rate is practically independent of the temperature effect.

The diminution of the E_{ap} values from low temperatures to high temperatures is consistent with an Arrhenius behavior [27,28]. The E_{ap} values found are in agreement with a change in the controlling reaction regime from chemical–mixed at low temperatures

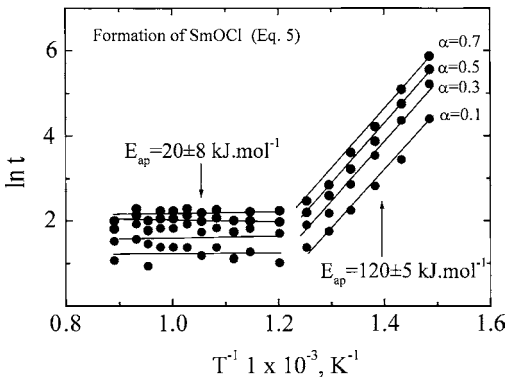

Fig. 12. Plot of $\ln t$ vs. T^{-1} at various conversions for 2 mg of Sm_2O_3+C between 400 and 850 °C. The stoichiometry considered corresponds to Eq. (5). β coefficient is 7.131 for this equation.

Table 3
Activation energy values of the formation of SmOCl and $SmCl_3$

Process	Temperature range (°C)	α range	E_{ap} (kJ mol^{-1})
SmOCl formation	400–525	0.10–0.90	120 ± 5
	525–850	0.10–0.90	20 ± 8
$SmCl_3$ formation	675–950	0.10–0.30	20 ± 8
	675–800	0.40–0.90	140 ± 5
	825–950	0.40–0.90	110 ± 10

to external mass transfer at high temperatures [25]. Although the direct chlorination of Sm_2O_3 presents similar E_{ap} values in the 525–850 °C range releasing SmOCl as a common product [20], neither the mass balances on the TG curves nor the attacks of the carbon surface confirm the influence of the direct chlorination on the carbochlorination. A resume of the E_{ap} values found is displayed in Table 3.

3.5.2. The formation of $SmCl_3$

The formation of $SmCl_3$ occurs as a second stage after that of SmOCl at temperatures higher than 650 °C. At this temperature, no total conversion of SmOCl to $SmCl_3$ is achieved. A mixture of both products is obtained, as observed in Fig. 8D.

At higher temperatures, between 675 and 950 °C, the chloride formed would be liquid, since the mp of $SmCl_3$ is 681 °C [18]. This would favor the mass transport of species what would make possible a more rapid and complete formation of $SmCl_3$ from SmOCl. At lower temperatures, the solid $SmCl_3$ formed over the solid SmOCl might not favor the transport of gas species and no complete reaction can be achieved.

Between 650 and 725 °C, the proposed two-stage scheme is given by Eq. (5) and

$$2SmOCl(s) + C(s) + 2Cl_2(g) \rightarrow 2SmCl_3(s, l) + CO_2(g) \quad (8)$$

and achieving the global stoichiometry shown in Eq. (6).At temperatures between 725 and 850 °C, the first stage coincides with the stoichiometry indicated on (5) but mass balances on the second stage are in agreement with the following reaction:

$$SmOCl(s) + C(s) + Cl_2(g) \rightarrow SmCl_3(s, l) + CO(g) \quad (9)$$

and achieving the global stoichiometry shown in Eq. (7).

As explained earlier, the stages proposed are confirmed by mass balances on the TG curves and XRD identification of the products. Although SmOCl is detected at temperatures higher than 850 °C and chemical attacks are observed at carbon surface at low reaction degrees, the processes influencing the reaction are competing for control and no exact stoichiometry can be assigned to the first step. Despite that, the complete formation of $SmCl_3$ is obtained in agreement to Eq. (7).

The calculation of the E_{ap} values assuming the global stoichiometry of (7) and (6) for the lower temperatures is displayed on Fig. 13. The values are calculated from 675 to 950 °C. Only those of $\alpha = 0.4$, 0.6, 0.7 and 0.9 are shown. The E_{ap} values found and their temperature and α ranges are resumed on Table 3.

3.5.2.1. E_{ap} values at α between 0.1 and 0.3. At these α values, the E_{ap} value is 20 ± 8 kJ mol^{-1}. It corresponds to the formation of SmOCl in the first stage. The E_{ap} values are similar to that of the formation of SmOCl at temperatures between 525 and 850 °C. This low E_{ap} value indicates external mass transfer control [25,26]. This conclusion is supported by Fig 11B where the effect of starvation at low α values is observed at 950 °C and by the comparison of Table 2

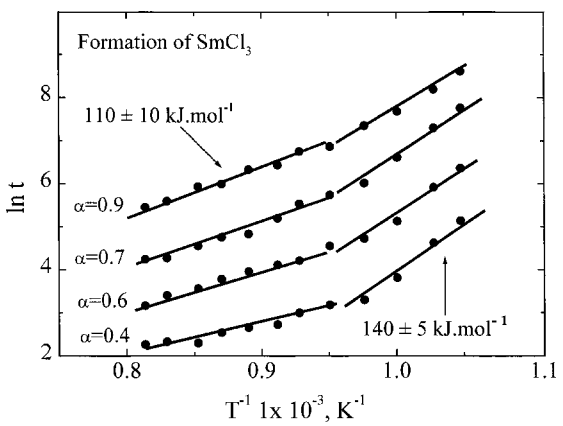

Fig. 13. Plot of $\ln t$ vs. T^{-1} at various conversions for 2 mg of Sm_2O_3 + C between 650 and 950 °C. The stoichiometries considered correspond to Eqs. (6) and (7). β coefficients are 2.71 and 2.37, respectively.

where both experimental and theoretical reaction rate values are of the same order [7,24].

3.5.2.2. E_{ap} values at α between 0.4 and 0.9. The E_{ap} value found is $140 \pm 5\,kJ\,mol^{-1}$ between 675 and 800 °C. The increment from $20 \pm 8\,kJ\,mol^{-1}$ at low reaction degrees to this value at high reaction degrees is associated to a change in the mechanism of reaction [25,29]. This change is related to the passage from the first to the second stage of reaction. This E_{ap} value at high reaction degrees is in agreement with a chemical–mixed control regime [25]. Nevertheless, the E_{ap} value is diminished as temperature is raised over 800 °C achieving a value of $110 \pm 10\,kJ\,mol^{-1}$ as observed in Fig. 13. This value also indicates chemical–mixed control regime [25]. Therefore, the diminution of the E_{ap} values observed is due to an increasing influence of external mass transfer on this chemical–mixed controlled stage [27]. This is consistent with a typical Arrhenius behavior [27]. It is supported by the conclusions obtained from Fig. 11B where this stage is found to be influenced by starvation [24] at the higher temperature and high α values.

4. Conclusions

The findings in this paper have improved the scarce knowledge on the carbochlorination of Sm_2O_3. The Sm_2O_3–C–Cl_2 is a complex system. Nevertheless, the systematic TG measurements allowed to find the stoichiometries of reaction in all the analyzed range. The effect of total gas flow rate and convective mass transfer were analyzed to estimate their influence on the reaction rate.

The effect of the temperature on the chlorination rate of Sm_2O_3(s)–C(s) mixture was evaluated from 200 to 950 °C. The starting temperature of carbochlorination is obtained at 400 °C. Between this temperature and 625 °C, one stage is obtained. At higher temperatures, the two consecutive stages of the reaction are evidenced. The first one leads to the formation of SmOCl and the second one to the formation of $SmCl_3$.

The E_{ap} value involved on the formation of SmOCl is of $120 \pm 5\,kJ\,mol^{-1}$ between 400 and 625 °C. At higher temperatures, the E_{ap} value is $20 \pm 8\,kJ\,mol^{-1}$.

The second stage produces $SmCl_3$ with the stoichiometries of Eq. (7) between 650 and 725 °C and Eq. (6) between 750 and 950 °C. The E_{ap} value found was $140 \pm 5\,kJ\,mol^{-1}$ between 675 and 800 °C. At higher temperatures, between 800 and 950 °C, the E_{ap} values of the second stage diminishes up to $110 \pm 10\,kJ\,mol^{-1}$. Although both E_{ap} values indicate chemical–mixed controlling regime [25], the change on the values is related to an increasing influence of external mass transfer as temperature is incremented on the mixed–chemical controlled step [27].

The complexity of this system is related to the intrinsic kinetics of the carbochlorination reactions [8,9,21,22]. These reactions release intermediates of reaction which mechanism of formation are not completely established. The influence of the carbon content on the reaction rate will be the next step on the study of the Sm_2O_3–C–Cl_2 system.

Acknowledgements

The authors wish to thank to the Agencia Nacional de Promoción Científica y Tecnológica (ANPCyT) of Argentina for the financial support of this work by PICT 00-109984 project.

References

[1] S. Cotton, Lanthanides and Actinides, Macmillan, London, 1991, p. 23.
[2] L. Mors, J. Less Common Met. 93 (1983) 301–321.
[3] T. Sato, Thermochim. Acta 148 (1989) 249–260.
[4] R.G. Haire, L. Eyring, Comparisons of the binary oxides, Handbook of the Physics and Chemistry of the Rare Earths, vol. 18, North-Holland, Amsterdam, 1994, Chapter 125, p. 439.
[5] C.K. Gupta, N. Krishnamurthy, Int. Mater. Rev. 37 (5) (1992) 197.
[6] M.R. Esquivel, A.E. Bohé, D.M. Pasquevich, in: J.P. Barbosa, A.J. Dutra, R. Melamed, R. Trindade (Eds.), Proceedings of the sixth Southern Hemisphere Meeting on Mineral Technology, vol. 2, 2001, pp. 468–474.
[7] M.R. Esquivel, A.E. Bohé, D.M. Pasquevich, Thermochim. Acta, in press.
[8] J.J.A. Gamboa, A.E. Bohé, D.M. Pasquevich, Thermochim. Acta 334 (1999) 131–139.
[9] D.M. Pasquevich, J.J.A. Gamboa, A. Caneiro, Thermochim. Acta 209 (1992) 209–222.
[10] W. Brugger, E. Greinacher, JOM (1967) 32–35.
[11] J. Gonzalez, M. Ruiz, A. Bohé, D.M. Pasquevich, Carbon 37 (1999) 1979–1988.

[12] S. Bernal, F.J. Botana, J. Pintado, R. García, J.M. Rodriguez Izquierdo, J. Less Common Met. 110 (1985) 439–443.
[13] Joint Committee for Powder Diffraction Standards, Powder Diffraction File, International Center for Diffraction Data, Swarthmore, PA, 1996 (Card number 150813).
[14] D.M. Pasquevich, A. Caneiro, Thermochim. Acta 156 (2) (1989) 275–283.
[15] D. Brown, Halides of the Lanthanides and Actinides, Wiley, London, 1968, p. 156.
[16] H.A. Heick, Lanthanide and actinide halides, Handbook of the Physics and Chemistry of Rare Earths, vol. 18, North-Holland, Amsterdam, 1994 (Chapter 124).
[17] S. Boghosian, G.N. Papatheodorou, Handbook of the Physics and Chemistry of Rare Earths, vol. 23, North-Holland, Amsterdam, 1996, Chapter 157, pp. 450–451.
[18] A. Roine, Outokumpu HSC Chemistry for Windows, 93001-ORGT, Version 2.0, Outokumpu Research Oy Information Service, Finland, 1994.
[19] Joint Committee for Powder Diffraction Standards, Powder Diffraction File, International Center for Diffraction Data, Swarthmore, PA, 1996 (Card number 120790).
[20] M.R. Esquivel, A.E Bohé, D.M. Pasquevich, Unpublished work.
[21] F.C. Gennari, A.E. Bohé, D.M. Pasquevich, Thermochim. Acta 3271 (1997) 1–9.
[22] J.R. Gonzalez, F.C. Gennari, M. Ruiz, A.E. Bohé, D.M. Pasquevich, Trans. Inst. Miner. Metall. C 107 (1998) C130–C138.
[23] Joint Committee for Powder Diffraction Standards, Powder Diffraction File, International Center for Diffraction Data, Swarthmore, PA, 1996 (Card number 120789).
[24] A.W. Hills, Metall. Trans. B 9B (1978) 121.
[25] F. Habashi, Principles of Extractive Metallurgy, vol. 1, Gordon and Breach, New York, 1969, Chapter 7, pp. 143–144.
[26] L.K. Doraiswamy, M.M. Sharma, Heterogeneous Reactions: Analysis, Examples and Reactor Design, vol. 1, Wiley, New York, 1984, Chapter 7, p. 143.
[27] L.K. Doraiswamy, M.M. Sharma, Heterogeneous Reactions: Analysis, Examples and Reactor Design, vol. 1, Wiley, New York, 1984, Chapter 7, p. 149.
[28] J. Szekely, J. Evans, H.Y. Sohn, Gas–Solid Reactions, Academic Press, New York, 1976, Chapter 4, pp. 109–110.
[29] O. Levenspiel, Chemical Reaction Engineering, Wiley, New York, 1979, p. 32.